ROYAL SOCIETY OPEN SCIENCE

rsos.royalsocietypublishing.org

Research

Article submitted to journal

Subject Areas:
foodwebs, paleontology, ecology

Keywords:
foodwebs, mammals, foraging

Author for correspondence:
Taran Rallings
e-mail: trallings@ucmerced.edu

Supplemental Materials: On the dynamics of starvation, mortality, and the ephemeral nature of mammalian megafauna

Taran Rallings[1], Christopher P Kempes[2], Justin D. Yeakel[1]

[1]School of Natural Sciences, University of California Merced
[2]Santa Fe Institute

THE ROYAL SOCIETY PUBLISHING

(a) Dimensional system to non-dimensionalized system

Recall that $\hat{k} = k/2$ where k is the resource carrying capacity. We begin with the dimensional consumer-resource system

$$\frac{dC_d}{dt} = \lambda_{\mathrm{C}} \frac{R_d}{\hat{k}} C_d - \sigma \left(1 - \frac{R_d}{k}\right) C_d,$$
$$\frac{dR_d}{dt} = \alpha R_d \left(1 - \frac{R_d}{k}\right) - \left(\frac{\lambda_{\mathrm{C}}^{\max}}{Y_{\mathrm{C}}} R_d + \rho\right) C_d. \tag{S0.1}$$

We define dimensionless variables $C = fC_d$, $R = qR_d$, and $t = st_d$, giving us

$$\frac{dC}{dt} = \frac{1}{s}\left[\lambda_{\mathrm{C}} \frac{R}{q\hat{k}} C - \sigma \left(1 - \frac{R}{qk}\right) C\right],$$
$$\frac{dR}{dt} = \frac{1}{s}\left[\alpha R \left(1 - \frac{R}{qk}\right) - \left(\frac{\lambda_{\mathrm{C}}}{Y_{\mathrm{C}} \hat{k} q} R + \rho\right) C\right]. \tag{S0.2}$$

We then set $s = 1$, $q = 1/k$, and $f = 1/Y_C \hat{k}$ to get

$$\frac{dC}{dt} = \lambda_{\mathrm{C}} \frac{R}{\hat{k}/k} C - \sigma (1 - R) C,$$
$$\frac{dR}{dt} = \alpha R (1 - R) - \left(\lambda_{\mathrm{C}} R_d + \frac{\rho Y_C \hat{k}}{k}\right) C. \tag{S0.3}$$

We then define the dimensionless parameters $\xi = k/\hat{k}$ and $\delta = \rho Y_C \hat{k}/k$ to get

$$\frac{dC}{dt} = \xi \lambda_{\mathrm{C}} RC - \sigma (1 - R) C,$$
$$\frac{dR}{dt} = \alpha R (1 - R) - (\lambda_{\mathrm{C}} R_d + \delta) C. \tag{S0.4}$$

(b) Derivation of allometric vital rates

(c) The influence of variations in model parameters and allometric rates

While our framework dictates that plant growth rates and carrying capacities are directly proportional to consumer steady states, we can gain insight into what drives the very large range of observed consumer densities by exploring the observed ranges of α and k in terrestrial systems. We assume an intrinsic growth rate roughly that of grass where $\alpha = 9.45 \times 10^{-9}$ (s^{-1}; REF), whereas observations among terrestrial plants reveal a range in growth rates from 2.81×10^{-10} to 2.19×10^{-8} [1], according with a change in α of roughly 97% lower and 130% higher than the set value. By incorporating this range into our the estimated resource growth rate, we observe that we can account for a large portion of consumer steady state densities around the mean density given by Eq. **??** (inner shaded region, Fig. **??**). If we additionally adjust the carrying capacity k of the resource to 90% less-than and 150% more-than the assumed value of 23×10^3 $\mathrm{g/m^2}$, our framework accounts for nearly the full range of mammalian steady state densities (outer shaded region, Fig. **??**). In this context, the upper-boundary of k observed to capture most higher herbivore densities is ca. 34 $\mathrm{kg/m^2}$, which is on the higher end of estimated live above-ground biomass densities in terrestrial forests such as in Isle Royal and the Allegheny National Forest [2].

Our model's ability to capture the bounds of mammalian densities at low and high productivity invites some speculation into the actual steepness of the mass-density relationship. While the best-fit slope to Damuth's Law is -0.77 (-0.74 using XX) we also observe that the steeper relationship given by our framework better captures the boundaries of mass-density data, whereas varying the intercept of the statistical best-fit would not capture the lower-density outer-boundary of larger species. While within-clade mass-density relationships often reveal a shallower slope than if measured across clades [3], it is possible that the absence of data for

larger mammals may bias estimates of the slope towards smaller (shallower) values. Mammalian communities have undergone significant anthropogenic restructuring throughout the Holocene (REF), such that many larger species are excluded from the mass-density relationship by way of extinction (REF), and the greater prevalence of smaller species may introduce size-dependent biases. For example, if species < 100 g are excluded, the empirical mass-density slope steepens from -0.77 to -0.85.

Considering how variations to the underlying energetic parameters driving consumer-resource dynamics alters the expected mass-density relationship may shed light on key constraints shaping mammalian communities. We next explore how variations in the vital rates included in the consumer-resource model modify the expected intercept and slope of the mammalian mass-density relationship. Different vital rates impact the mass-density relationship in three distinct ways, by either *i*) influencing only the mass-density slope, *ii*) influencing only the mass-density intercept, or *iii*) influencing both. Aside from the resource growth rate and carrying capacity, our framework also includes the intrinsic consumer reproductive rate $\lambda_C^{\max}$, the consumer yield coefficient Y_C, and the maximum rate of starvation σ. We introduce changes to these rates as, for example, $\lambda_C^{\max\prime} = \lambda_C^{\max}(1+\chi)$, where $\chi \in (-1, 2)$ represents the proportion increase or decrease of the altered parameter denoted by $'$. We note that the recovery rate ρ is sufficiently small that alterations do not have an influence on either the consumer mass-density intercept or slope.

Importantly, changes to the starvation rate have a large effect on both the consumer-density intercept and slope (Fig. **??**E,F). We observe that decreasing σ from the expected value ($\chi < 0$) serves to increase the steady state intercept, while decreasing the mass-density slope. By comparison, increasing σ from the expected value ($\chi > 0$) has less effect on the mass-density relationship. In the consumer-resource model described in Eq. **??**, starvation is the sole source of consumer mortality, and therefore plays an out-sized role in determining consumer steady states. As this mortality is reduced, consumer densities increase, raising the intercept. However, as consumer starvation rates decline we observe a steeper mass-density slope. Reduced starvation rates therefore principally benefit the steady state densities of smaller species, with reduced effects observed for larger-bodied mammals. Because fat biomass scales super-linearly with body mass (see methods; REFS), the populations of larger consumers are more resilient to the effects of starvation, whereas those of smaller consumers are more prone.

The consumer's maximal rate of reproduction $\lambda_C^{\max}$ influences only the mass-density slope except for the case $\chi \to -1$, where growth becomes zero. Above this trivial limit, we observe the consumer growth rate to have a negative effect on the mass-density slope, such that as the growth rate increases, the mass-density relationship becomes steeper (Fig. **??**A,B). As the intercept does not change, this means that the steady states of larger bodied consumers decline with increasing $\lambda_C^{\max}$, while those of smaller-bodied consumers remain unaltered, though the effect is slight. Of more interest is the effect of the yield coefficient Y_C and starvation rate σ (Fig. **??**C-F). The yield coefficient represents the conversion of resources to consumer biomass, where an increase in χ correlates to large increases in consumer steady state without altering the mass-density slope. Here we observe that increased efficiency in converting resource to consumer biomass will have an effect similar to increasing resource productivity, as the effective abundance of the resource is greater when relatively fewer resources fuel a given unit of consumer biomass. Because $Y_C \propto E_d$ where E_d is the energy density of the resource (see methods), resource quality is therefore expected to translate directly to higher consumer steady state densities.

(d) Derivation of allometric natural mortality

(e) Derivation of allometric capture rates

(f) Derivation of harvesting mortality

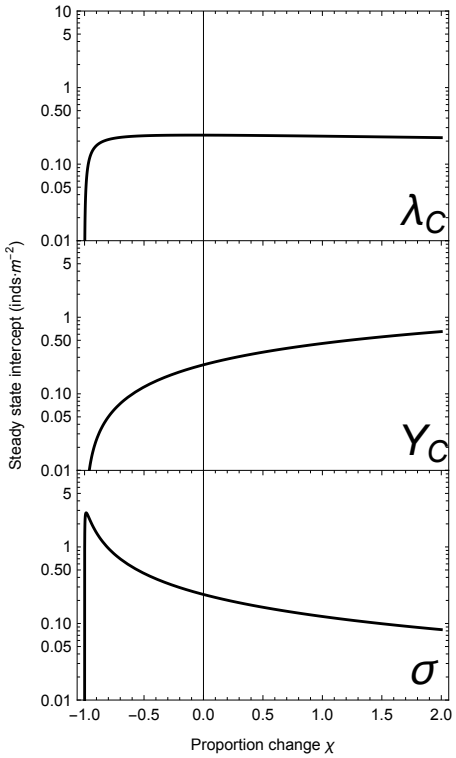

Figure S1: The effects of changes to metabolic parameters on the prediction of the mass-density relationship.

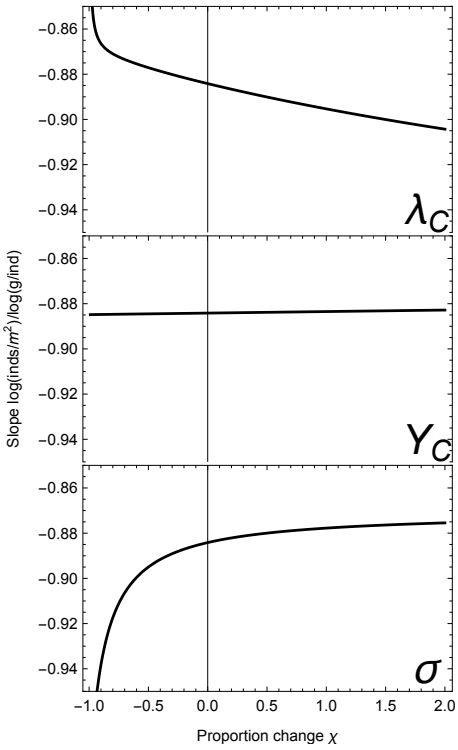

Figure S2: The effects of changes to metabolic parameters on the prediction of the mass-density relationship.

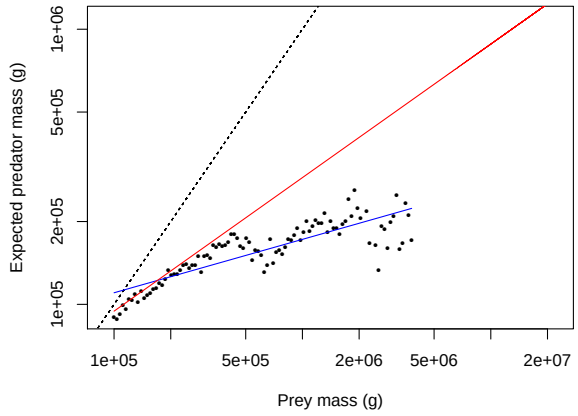

Figure S3: Expected predator masses for contemporary large-bodied ($> 10^5$ g) terrestrial predators and prey. Expected predator sizes as a function of herbivore size class were determined by reconstructing dietary samples from observed trophic interactions for cheetah, wild dogs, dholes, leopards, hyenas, lions, and tigers from [4] (REF others), where masses for both predators and prey were allowed to vary $\pm 20\%$ from measured estimates. The blue line denotes the best fit relationship, given by $\mathrm{E}(M_P|M_C) = p_0 M_C^{p_1}$, where $p_0 = 11786.8$ g and $p_1 = 0.194$. The red line represents a modified PPMR where $p_0' = p_0(1 + \chi_{\mathrm{int}})$ and $p_1' = p_1(1 + \chi_{\mathrm{slope}})$ where $\chi_{\mathrm{int}} = 0.97$ and $\chi_{\mathrm{slope}} = 1.50$ that allows megatrophic interactions and resides within the white band displayed in Fig. **??**C,D. This relationship is entirely hypothetical, but does not stray far from observations of contemporary species, describes megapredators that predate on megaherbivores, and results in threshold herbivore and carnivore size classes that permit dynamically feasible megatrophic interactions. The black line denotes the 1:1 line.

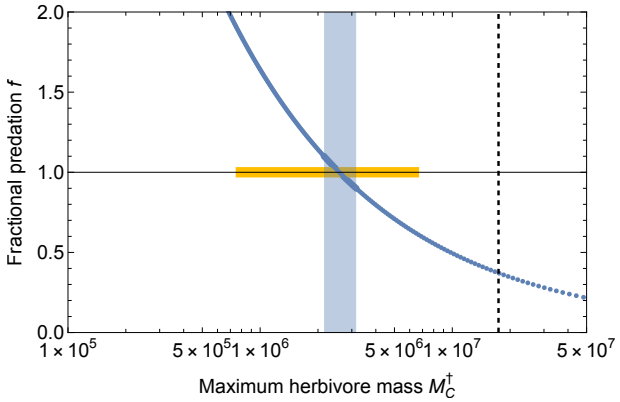

Figure S4: The effect of changing the reliance of predator growth f on the single herbivore consumer population. If $f = 1$, the predator solely relies on the herbivore consumer. If $0 < f < 1$, the predator relies on the herbivore population to support a fraction of its growth. If $f > 1$, the predator is removing more biomass than is necessary to support its growth. Blue region denotes herbivore threshold mass range characterizing $f = 1 \pm 0.1$. Yellow line denotes the mass range of contemporary elephants. Vertical dashed line denotes the size of the largest terrestrial mammal (Deinotherium at ca. 1.74×10^7, corresponding to $f = 0.37$, such that a predator is supporting a little more than $1/3$ of its growth from the herbivore consumer.

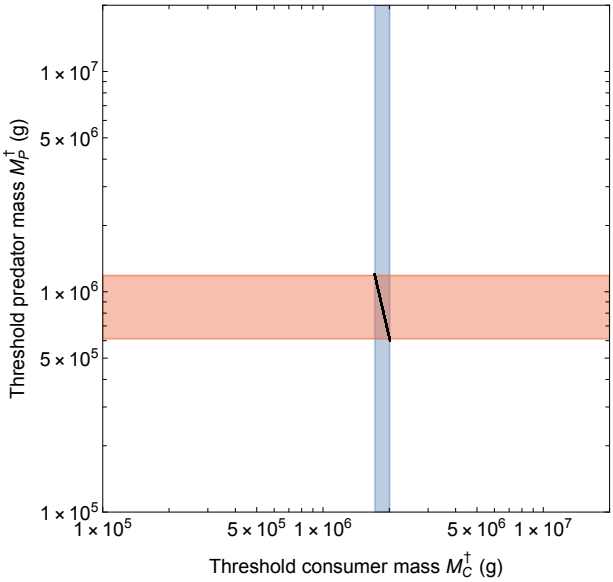

Figure S5: Mass ranges corresponding to feasible megatrophic interactions (where herbivore and predator threshold masses are $> 6 \times 10^5$ g) across variations to the assumed predator-prey mass ratio (PPMR), demarcated by the white bands in Fig. **??**C,D, and under the assumption specialist predation ($f = 1$).

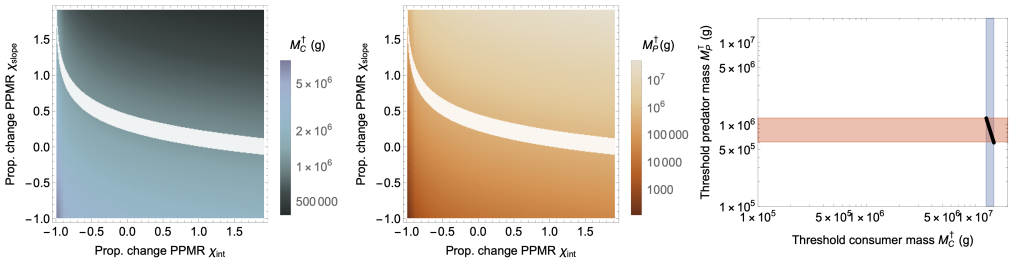

Figure S6: The effects of predator generalization on A) threshold herbivore mass $M_C^\dagger$ and B) threshold predator mass $M_P^\dagger$ across variable PPMRs, where $\mathrm{E}(M_P|M_C) = p_0(1 + \chi_{\mathrm{int}})M_C^{p_1(1+\chi_{\mathrm{slope}})}$ and both χ_{int} and $\chi_{\mathrm{slope}} \in (-0.99, 2)$. White bands denote regions of χ_{int} and χ_{slope} where megatrophic interactions are feasible (both perdator and herbivore threshold masses are $> 6 \times 10^5$ g). C) Mass ranges corresponding to feasible megatrophic interactions in the white bands in A and B.

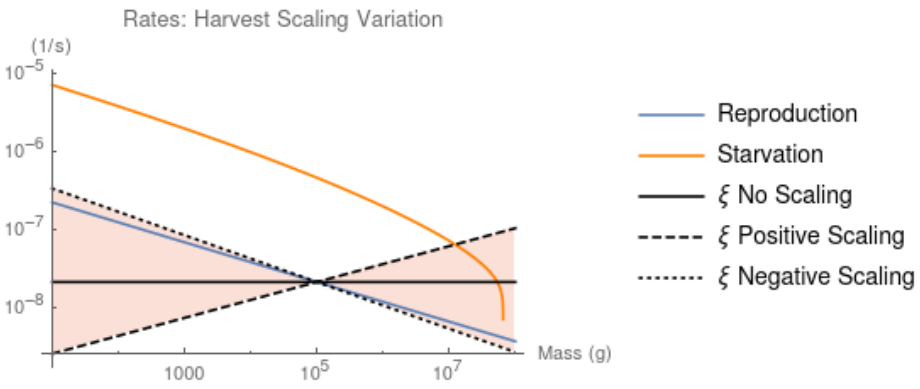
Rates: Harvest Scaling Variation
(1/s)
10^{-5}
10^{-6}
10^{-7}
10^{-8}
1000
10^5
10^7
Mass (g)
Reproduction
Starvation
ξ No Scaling
ξ Positive Scaling
ξ Negative Scaling

Figure S7

References

1. Michaletz ST, Cheng D, Kerkhoff AJ, Enquist BJ. 2014 Convergence of terrestrial plant production across global climate gradients. *Nature* **512**, 39–43.
2. De Jager NR, Drohan PJ, Miranda BM, Sturtevant BR, Stout SL, Royo AA, Gustafson EJ, Romanski MC. 2017 Simulating ungulate herbivory across forest landscapes: A browsing extension for LANDIS-II. *Ecological Modelling* **350**, 11–29.
3. Pedersen RØ, Faurby S, Svenning JC. 2017 Shallow size–density relations within mammal clades suggest greater intra-guild ecological impact of large-bodied species. *J. Anim. Ecol.* **86**, 1205–1213.
4. Hayward MW, Kerley G. 2008 Prey preferences and dietary overlap amongst Africa's large predators. *S. African J. Wild. Res.* **38**, 93–108.